



**HAL**  
open science

# A Detailed Study on a DC-Voltage-Based Control Scheme Using a Multi-Terminal HVDC System for Frequency Control

Yijing Chen, Jing Dai, Gilney Damm, Françoise Lamnabhi-Lagarrigue

► **To cite this version:**

Yijing Chen, Jing Dai, Gilney Damm, Françoise Lamnabhi-Lagarrigue. A Detailed Study on a DC-Voltage-Based Control Scheme Using a Multi-Terminal HVDC System for Frequency Control. 12th European Control Conference (ECC 2013), Jul 2013, Zurich, Switzerland. pp.3530–3535, 10.23919/ecc.2013.6669663. hal-00826026

**HAL Id: hal-00826026**

**<https://centralesupelec.hal.science/hal-00826026>**

Submitted on 30 Mar 2021

**HAL** is a multi-disciplinary open access archive for the deposit and dissemination of scientific research documents, whether they are published or not. The documents may come from teaching and research institutions in France or abroad, or from public or private research centers.

L'archive ouverte pluridisciplinaire **HAL**, est destinée au dépôt et à la diffusion de documents scientifiques de niveau recherche, publiés ou non, émanant des établissements d'enseignement et de recherche français ou étrangers, des laboratoires publics ou privés.

# A Detailed Study on a DC-Voltage-Based Control Scheme Using a Multi-Terminal HVDC System for Frequency Control

Yijing Chen<sup>1</sup>, Jing Dai<sup>1</sup>, Gilney Damm<sup>2</sup>, Françoise Lamnabhi-Lagarrigue<sup>1</sup>

**Abstract**—This paper investigates a control strategy that uses a multi-terminal high voltage direct current (HVDC) system for frequency control. It first describes a DC voltage control law which, based only on local information, makes the interconnected non-synchronous systems share their primary reserves. Then, a sufficient condition for choosing the controller gains is developed based on Lyapunov theory and LMI techniques with rigorous mathematical stability proofs. Simulation results show that the control strategy has achieved the objective of sharing primary reserves, guarantees the whole system's ultimate boundedness and improves the transient and steady-state performance.

## I. INTRODUCTION

Nowadays the world total electricity demand increases year by year while the existing alternating current (AC) transmission grids are operated close to their limits. As it is difficult to upgrade the existing AC grids, high voltage direct current (HVDC) is considered as an alternative solution. HVDC transmission systems [1] use direct current for bulk power transmission. They are suitable for long-distance bulk transmission, underground and submarine cable transmission, asynchronous interconnection, etc. From an economic point of view, HVDC transmission systems are more attractive than their AC counterpart for long-distance power delivery and high power ratings. On the other hand, the traditional two-terminal HVDC systems can only carry out point-to-point power transmission. However, for economic and technological reasons, it is necessary to study the grids connecting several power sources and consumers. For this, multi-terminal HVDC (MTDC) could be a good solution. Unfortunately, the results on multi-terminal systems are rare.

In an AC system the frequency, as an indication of power balance, is common everywhere on the time scale of a few milliseconds. With this common frequency, all generating units within the system can sense a power imbalance and adjust their power output to counter this disturbance. This mechanism of restoring power balance is commonly called primary frequency control, and the region of variation of generators' output is referred to as primary reserve. However, with the current practice of transferring a scheduled power among the AC areas through HVDC links, the frequencies of the areas are independent of each other, and thus generators

in one area are not sensible to other areas' power imbalances. The advantage of this practice is that a disturbance in one area does not affect another, and thus the HVDC link can play the role of a firewall to prevent cascading failure. However, in the case of a severe power imbalance, the generating units within the affected area may not be strong enough to restore the power balance in time, and the resulting frequency excursion may be so large that invasive and expensive corrective measures (e.g. load shedding) have to be triggered. Such undesirable scenarios may be avoided if the HVDC system can be controlled in real time in such a way that the interconnected AC areas can share their primary reserves.

References [2], [3] proposed frequency controllers that modify the active power transferred by an HVDC link. However, these proposed controllers require other AC areas' frequency measurements. Due to the time-delay of information communication, the controllers may destabilize the overall system. To become independent of remote information [4] proposes a controller, named the DC-voltage-based controller, which takes actions only based on local information, requiring no communication among the AC areas. However, the theoretical stability proof in [4] is only valid for the special case of identical parameters of the AC areas, which is unrealistic in practice. In addition, the choice of the controller gain in [4] was also rather empirical, and no proper approach to tuning the controller gain was given.

In this paper, we study a more general case without any restrictions on AC areas' parameters. A rigorous stability analysis is given to ensure safety and reliability. Moreover, we investigate the feasible region for the controller gains based on Lyapunov theory (see [5], [6], [7], [8]) and LMI techniques [9].

The paper is organized as follows: Section II presents an MTDC system and introduces a simplified model. Section III describes the control strategy, gives theoretical stability proof and presents an approach to establish the controller gain that guarantees the reliability of the system. The performance is illustrated by simulation results in Section IV. Section V presents the conclusions.

## II. MULTI-TERMINAL HVDC SYSTEM MODEL

In this paper, we consider a special network where each AC area is connected by only one converter. A simplified MTDC system consisting of a DC grid,  $N$  AC areas, and  $N$  VSC converters, is shown in Fig. 1, where  $P_i^{dc}$  represents DC power injections to the HVDC grid. If  $P_i^{dc}$  is negative,

This work is supported by WINPOWER project.

<sup>1</sup>Y. Chen, J. Dai and F. Lamnabhi-Lagarrigue are with Laboratoire des Signaux et Systèmes (LSS), Supélec, 3 rue Joliot-Curie, 91192 Gif-sur-Yvette, France (tel: +33 1 69 85 17 77, e-mail: yijing.chen@lss.supelec.fr, jing.dai@supelec.fr, francoise.lamnabhi-lagarrigue@lss.supelec.fr).

<sup>2</sup>G. Damm is with Laboratoire IBISC, Université d'Evry-Val d'Essonne, 40 rue du Pelvoux, 91020 Evry, France (e-mail: gilney.damm@ibisc.fr).

AC area  $i$  absorbs power from the HVDC grid as a consumer. Otherwise, AC area  $i$  provides power as a supplier.

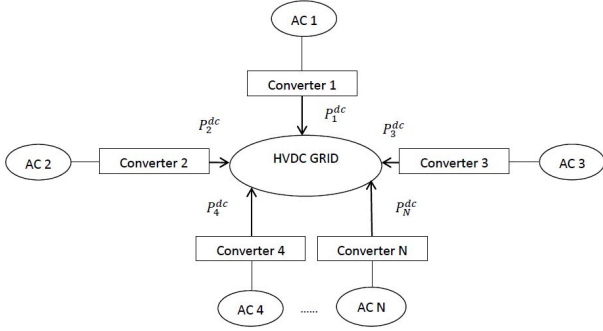


Fig. 1. Diagram of an MTDC system with  $N$  AC areas.

### A. DC grid

Each DC voltage is denoted as  $V_i$ . All converters can independently control their  $V_i$  thanks to VSC converter and PWM technology. The power injected to the DC grid from AC area  $i$ ,  $P_i^{dc}$ , satisfies Ohm's law

$$P_i^{dc} = \sum_{k=1}^N \frac{V_i(V_i - V_k)}{R_{ik}}, \quad (1)$$

where  $R_{ik}$  is the resistance between AC areas  $i$  and  $k$ . Obviously  $R_{ik} = R_{ki}$ . If AC areas  $i$  and  $k$  are not connected directly,  $R_{ik}$  is infinity.

### B. AC areas

Each AC area is modeled as an aggregated generator and a load. The equation of motion of the generator is

$$2\pi J_i \frac{df_i}{dt} = \frac{P_{mi} - P_{li} - P_i^{dc}}{2\pi f_{nom,i}} - 2\pi D_{gi}(f_i - f_{nom,i}), \quad (2)$$

where  $P_{mi}$ ,  $J_i$  and  $D_{gi}$  are the mechanical power input, the moment of inertia and the damping factor of the aggregated generator of area  $i$ , respectively.  $f_i$  is the frequency of AC area  $i$  and  $f_{nom,i}$  is its nominal value.  $P_{li}$  is the power consumed by area  $i$ 's load.  $J_i$ ,  $D_{gi}$  and  $f_{nom,i}$  are considered as known parameters.

The primary frequency control is realized by the speed governor of the generator, which modifies  $P_{mi}$  in response to a deviation of  $f_i$  from  $f_{nom,i}$ . This dynamics is modeled as

$$T_{sm,i} \frac{dP_{mi}}{dt} = P_{mi}^o - P_{mi} - \frac{P_{nom,i}}{\sigma_i} \frac{f_i - f_{nom,i}}{f_{nom,i}}, \quad (3)$$

where  $T_{sm,i}$  is the time constant of the servomotor,  $P_{mi}^o$  is the reference value for  $P_{mi}$ ,  $P_{nom,i}$  is the nominal power of the generator and  $\sigma_i$  is the generator droop.

By combining (2) and (3), the whole system is represented as

$$\begin{cases} 2\pi J_i \frac{df_i}{dt} = \frac{P_{mi} - P_{li} - P_i^{dc}}{2\pi f_{nom,i}} - 2\pi D_{gi}(f_i - f_{nom,i}), \\ T_{sm,i} \frac{dP_{mi}}{dt} = P_{mi}^o - P_{mi} - \frac{P_{nom,i}}{\sigma_i} \frac{f_i - f_{nom,i}}{f_{nom,i}}, \end{cases} \quad (4)$$

for  $i = 1, \dots, N$ .  $f_i$  and  $P_{mi}$  are the state variables. By substituting (1) into (4),  $V_i$  explicitly appear in the system model, and they are considered as the control inputs.

### C. Reference operating point

We define the reference operating point as follows. It is a steady-state defined by specific values of input parameters  $P_{li}$ ,  $P_{mi}^o$  and the variables  $f_i$ ,  $P_{mi}$ ,  $P_i^{dc}$ ,  $V_i$ . Denote by  $\bar{P}_{li}$ ,  $\bar{P}_{mi}^o$ ,  $\bar{f}_i$ ,  $\bar{P}_i^{dc}$ ,  $\bar{P}_{mi}$ ,  $\bar{V}_i$  the reference operating point values.

In this paper, the values of  $\bar{f}_i$  and  $\bar{P}_{mi}$  at the reference operating point equal their nominal values, i.e.

$$\bar{f}_i = f_{nom,i}, \quad \forall i \in \{1, 2, \dots, N\}, \quad (5)$$

$$\bar{P}_{mi} = P_{mi}^o, \quad \forall i \in \{1, 2, \dots, N\}. \quad (6)$$

Since the reference operating point is a steady state, we have

$$\begin{cases} 0 = \frac{\bar{P}_{mi} - \bar{P}_{li} - \bar{P}_i^{dc}}{2\pi f_{nom,i}} - 2\pi D_{gi}(\bar{f}_i - f_{nom,i}), \\ 0 = P_{mi}^o - \bar{P}_{mi} - \frac{P_{nom,i}}{f_{nom,i}} \frac{\bar{f}_i - f_{nom,i}}{\sigma_i}, \\ \bar{P}_i^{dc} = \sum_{k=1}^N \frac{\bar{V}_i(\bar{V}_i - \bar{V}_k)}{R_{ik}}. \end{cases} \quad (7)$$

$\bar{V}_i$  is obtained by solving (7).

## III. CONTROL STRATEGY

Consider that the MTDC system initially operates at the reference operating point. Then, one of its AC areas is subjected to a disturbance that takes form of a step load change, i.e.  $P_{li} \neq \bar{P}_{li}$ . It is true that this load change can be satisfied by the primary frequency control of its own area ( $P_{mi}$ ). However, in case of a large disturbance, if we rely only on  $P_{mi}$ , the resulting frequency deviation may be so large that it endangers the correct operation of the system. Thus, our objective is to improve the transient frequency profile by calling for other area's primary reserves so that the frequency excursions are less pronounced.

### A. Control law

The control objective is to regulate each converter's DC voltage  $V_i$  only based on local measurements  $f_i$ , i.e.  $V_i$  is a function of  $f_i$  only. Therefore, a DC voltage based controller is designed as

$$V_i = \bar{V}_i + \alpha_i(f_i - \bar{f}_i), \quad (8)$$

with positive gain  $\alpha_i > 0$ .

Under this controller, due to the physical coupling of the HVDC grid (1), the resulting power injected to DC grid  $P_i^{dc}$  can be regulated by controlling  $V_i$ . This method leads our whole system to achieve the objective of sharing every area's primary reserve. However, we are not sure whether  $f_i$  and  $P_{mi}$  are ultimately bounded around the reference operating point under the control law (8) with an arbitrary positive control gain  $\alpha_i$ .

## B. Choice of control gains

In this part, we give a detailed analysis for choosing the control gain  $\alpha_i$  to guarantee ultimate boundedness of  $f_i$  and  $P_{mi}$  under (8).

To simplify our problem, at first, we shift the reference values to the origins by introducing the following new variables:  $\tilde{P}_i^{dc} = P_i^{dc} - \bar{P}_i^{dc}$ ,  $\tilde{P}_{li} = P_{li} - \bar{P}_{li}$  and  $\tilde{V}_i = V_i - \bar{V}_i$ .

Equation (1) can be expressed in these new variables as

$$\tilde{P}_i^{dc} = \sum_{k \neq i}^N \frac{(\tilde{V}^2 + 2\tilde{V}_i \tilde{V}_k - \tilde{V}_i \tilde{V}_k - \tilde{V}_i \tilde{V}_k - \tilde{V}_k \tilde{V}_i)}{R_{ik}}. \quad (9)$$

We write (4) in terms of the new variables by combining (7) and (9)

$$\begin{cases} \dot{\tilde{f}}_i = -a_{1i} \tilde{f}_i + a_{2i} \tilde{P}_{mi} - a_{2i} \tilde{P}_{li} - a_{2i} \cdot \\ \quad \left( \sum_{k \neq i}^N \frac{\tilde{V}_i^2 + 2\tilde{V}_i \tilde{V}_k - \tilde{V}_i \tilde{V}_k - \tilde{V}_i \tilde{V}_k - \tilde{V}_k \tilde{V}_i}{R_{ik}} \right), \\ \dot{\tilde{P}}_{mi} = -a_{4i} \tilde{f}_i - a_{5i} \tilde{P}_{mi}, \end{cases} \quad (10)$$

where  $a_{1i} = \frac{D_{gi}}{J_i}$ ,  $a_{2i} = \frac{1}{4\pi^2 J_i f_{nom,i}}$ ,  $a_{4i} = \frac{P_{nom,i}}{T_{sm,i} \sigma_i f_{nom,i}}$ ,  $a_{5i} = \frac{1}{T_{sm,i}}$ . It is noted that  $a_{1i}$ ,  $a_{2i}$ ,  $a_{4i}$ ,  $a_{5i}$  are strictly positive, and that the control input  $\tilde{V}_i$  explicitly appears in the system.

$\tilde{P}_{li}$  can be considered as a nonvanishing perturbation which is uniformly bounded if a load demand imbalance exists, i.e.  $P_{li} - \bar{P}_{li} \neq 0$ . We think of the system (10) as a perturbation of the nominal system:

$$\begin{cases} \dot{\tilde{f}}_i = -a_{1i} \tilde{f}_i + a_{2i} \tilde{P}_{mi} - a_{2i} \cdot \\ \quad \left( \sum_{k \neq i}^N \frac{\tilde{V}_i^2 + 2\tilde{V}_i \tilde{V}_k - \tilde{V}_i \tilde{V}_k - \tilde{V}_i \tilde{V}_k - \tilde{V}_k \tilde{V}_i}{R_{ik}} \right), \\ \dot{\tilde{P}}_{mi} = -a_{4i} \tilde{f}_i - a_{5i} \tilde{P}_{mi}. \end{cases} \quad (11)$$

We know that, if the origin of the nominal system (11) is asymptotically stable under the control law, then the perturbed system (10) is ultimately bounded around the origin. Thus, the problem becomes to investigate a feasible region for  $\alpha_i$  such that the nominal system (11) is asymptotically stabilized around the origin under (8). In the following part, two methods are used to get a feasible region for  $\alpha_i$  by means of analyzing the stability of the nonlinear system (11).

1) *First approach - Linearization of injected DC power flow*: The first approach is to analyze the stability of the nonlinear system via linearization.

Linearizing (9) around the reference operating point leads to

$$\begin{aligned} \tilde{P}_i^{dc} &= \sum_{k \neq i}^N \frac{2\tilde{V}_i - \tilde{V}_k}{R_{ik}} \tilde{V}_i - \sum_{k \neq i}^N \frac{\tilde{V}_i}{R_{ik}} \tilde{V}_k \\ &= \sum_{k \neq i}^N \frac{\tilde{V}_i - \tilde{V}_k}{R_{ik}} \tilde{V}_i + \sum_{k \neq i}^N \frac{\tilde{V}_i}{R_{ik}} \tilde{V}_i - \sum_{k \neq i}^N \frac{\tilde{V}_i}{R_{ik}} \tilde{V}_k. \end{aligned} \quad (12)$$

Let  $\tilde{f} = [\tilde{f}_1, \tilde{f}_2, \dots, \tilde{f}_N]^T$ ,  $\tilde{P}_m = [\tilde{P}_{m1}, \tilde{P}_{m2}, \dots, \tilde{P}_{mN}]^T$ ,  $\tilde{P}^{dc} = [\tilde{P}_1^{dc}, \tilde{P}_2^{dc}, \dots, \tilde{P}_N^{dc}]^T$ ,  $\tilde{V} = [\tilde{V}_1, \tilde{V}_2, \dots, \tilde{V}_N]^T$ .

Equation (12) written in vector form becomes

$$\begin{aligned} \tilde{P}^{dc} &= \text{diag}(\tilde{V}_i) L \tilde{V} + \text{diag}(\tilde{V}_i) \text{diag} \left( \sum_{k \neq i}^N \frac{1}{R_{ik}} \right) \tilde{V} \\ &\quad - \text{diag} \left( \sum_{k \neq i}^N \frac{\tilde{V}_k}{R_{ik}} \right) \tilde{V}, \end{aligned} \quad (13)$$

where  $L \in \mathbb{R}^{N \times N}$  is the weighted Laplacian matrix describing the topology of HVDC grid, defined as

$$[L]_{ik} = \begin{cases} -\frac{1}{R_{ik}} & : k \neq i, \\ \sum_{j \neq i}^N \frac{1}{R_{ij}} & : k = i. \end{cases}$$

Let  $V = \text{diag}(\tilde{V}_i)$ ,  $R = \text{diag}(\sum_{k \neq i}^N \frac{1}{R_{ik}})$ ,  $V_R = \text{diag}(\sum_{k \neq i}^N \frac{\tilde{V}_k}{R_{ik}})$ . The nominal system (11) is expressed in matrix form as

$$\begin{bmatrix} \dot{\tilde{f}} \\ \dot{\tilde{P}}_m \end{bmatrix} = \begin{bmatrix} -A_1 & A_2 \\ -A_4 & -A_5 \end{bmatrix} \begin{bmatrix} \tilde{f} \\ \tilde{P}_m \end{bmatrix} - \begin{bmatrix} A_2(VL + VR - V_R) \\ 0 \end{bmatrix} \tilde{V}, \quad (14)$$

with

$$\tilde{V} = [A_\alpha \quad 0] \begin{bmatrix} \tilde{f} \\ \tilde{P}_m \end{bmatrix}, \quad (15)$$

where  $A_1 = \text{diag}(a_{1i})$ ,  $A_2 = \text{diag}(a_{2i})$ ,  $A_4 = \text{diag}(a_{4i})$ ,  $A_5 = \text{diag}(a_{5i})$ ,  $A_\alpha = \text{diag}(\alpha_i)$ .

By substituting (15) into (14), the closed-loop system is

$$\begin{bmatrix} \dot{\tilde{f}} \\ \dot{\tilde{P}}_m \end{bmatrix} = A \begin{bmatrix} \tilde{f} \\ \tilde{P}_m \end{bmatrix}, \quad (16)$$

where  $A = \begin{bmatrix} -A_1 - A_2(VL + VR - V_R)A_\alpha & A_2 \\ -A_4 & -A_5 \end{bmatrix}$ .

A Lyapunov-based method is used to find a feasible region for  $A_\alpha$ . Choose a Lyapunov function  $W$  as

$$W = \tilde{f}^T A_4 \tilde{f} + \tilde{P}_m^T A_2 \tilde{P}_m. \quad (17)$$

The derivative of  $W$  is

$$\dot{W} = -\tilde{f}^T F_\alpha \tilde{f} - 2\tilde{P}_m^T A_5 A_2 \tilde{P}_m, \quad (18)$$

where  $F_\alpha = 2A_1 A_4 + A_\alpha(LV + RV - V_R)A_2 A_4 + A_4 A_2(VL + VR - V_R)A_\alpha$ . Furthermore,  $F_\alpha$  is a symmetric matrix.

If there is a region for  $A_\alpha$  to make  $F_\alpha$  positive definite, the closed-loop system (16) is asymptotically stable. Thus, our problem becomes to find a feasible region for  $\alpha$  such that  $F_\alpha > 0$ , which is a linear matrix inequality (LMI). The objective is now to find a diagonal  $A_\alpha$  in order to rely only on local measurements. For this, we solve

$$\begin{cases} A_\alpha > 0, \\ 2A_1 A_4 + A_\alpha(LV + RV - V_R)A_2 A_4 \\ \quad + A_4 A_2(VL + VR - V_R)A_\alpha > 0. \end{cases} \quad (19)$$

The above LMI problem can be solved for typical values. As seen in (19), the feasible region for  $A_\alpha$  is determined by all the AC areas parameters and the reference operating point.

2) *Second approach - Nonlinear system:* It is well known that we can approximate the nonlinear system (11) by its linearized system (14) only in a neighbourhood of the origin [5]. Thus, to study the global behaviour of the system under the control law, we use a second approach to investigate directly the stability of the nonlinear system.

The same Lyapunov function as the linear case is chosen

$$W = \sum_{i=1}^N a_{4i} \tilde{f}_i^2 + \sum_{i=1}^N a_{2i} \tilde{P}_m^2. \quad (20)$$

We write (9) in vector form

$$\tilde{P}_i^{dc} = \text{diag}(\tilde{V}_i) L \tilde{V} + \text{diag}(\tilde{V}_i) L \bar{V} + \text{diag}(\tilde{V}_i) L \tilde{V}, \quad (21)$$

where  $\bar{V} = [\bar{V}_1, \dots, \bar{V}_N]^T$ .

The system (11) can be rewritten as

$$\begin{bmatrix} \dot{\tilde{f}} \\ \dot{\tilde{P}}_m \end{bmatrix} = \begin{bmatrix} -A_1 & A_2 \\ -A_4 & -A_5 \end{bmatrix} \begin{bmatrix} \tilde{f} \\ \tilde{P}_m \end{bmatrix} - \begin{bmatrix} A_2 \\ 0 \end{bmatrix} \cdot (\text{diag}(\tilde{V}_i) L \tilde{V} + \text{diag}(\tilde{V}_i) L \bar{V} + \text{diag}(\tilde{V}_i) L \tilde{V}), \quad (22)$$

with the control law:  $\tilde{V}_i = \alpha_i \tilde{f}_i$ , i.e.  $\text{diag}(\tilde{V}_i) = A_\alpha \text{diag}(\tilde{f}_i)$ . Then the closed-loop system is

$$\begin{bmatrix} \dot{\tilde{f}} \\ \dot{\tilde{P}}_m \end{bmatrix} = \begin{bmatrix} -A_1 & A_2 \\ -A_4 & -A_5 \end{bmatrix} \begin{bmatrix} \tilde{f} \\ \tilde{P}_m \end{bmatrix} - \begin{bmatrix} H_1(\tilde{f}) & 0 \\ 0 & 0 \end{bmatrix} \begin{bmatrix} \tilde{f} \\ \tilde{P}_m \end{bmatrix} - \begin{bmatrix} H_2(\tilde{f}) \\ 0 \end{bmatrix}, \quad (23)$$

where  $H_1(\tilde{f}) = A_2 A_\alpha \text{diag}(\tilde{f}_i) L A_\alpha + A_2 \text{diag}(\tilde{V}_i) L A_\alpha$  and  $H_2(\tilde{f}) = A_2 A_\alpha \text{diag}(\tilde{f}_i) L \bar{V}$ .

The derivative of Lyapunov function is

$$\dot{W} = -2\tilde{f}^T A_1 A_4 \tilde{f} - \tilde{f}^T A_4 H_1 \tilde{f} - \tilde{f}^T H_1^T A_4 \tilde{f} - \tilde{f}^T A_4 H_2 - H_2^T A_4 \tilde{f} - 2\tilde{P}_m^T A_5 A_2 \tilde{P}_m, \quad (24)$$

where

$$\tilde{f}^T A_4 H_1 \tilde{f} = \sum_{i=1}^N a_{4i} a_{2i} (\alpha_i \tilde{f}_i^2 + \bar{V}_i \tilde{f}_i) \left( \sum_{k \neq i}^N \frac{\alpha_i \tilde{f}_i - \alpha_k \tilde{f}_k}{R_{ik}} \right), \quad (25)$$

$$\tilde{f}^T A_4 H_2 = \sum_{i=1}^N a_{4i} a_{2i} \alpha_i \tilde{f}_i^2 \left( \sum_{k \neq i}^N \frac{\bar{V}_i - \bar{V}_k}{R_{ik}} \right). \quad (26)$$

We rewrite  $\dot{W}$  as

$$\dot{W} = -M_1 - M_2 - 2\tilde{P}_m^T A_5 A_2 \tilde{P}_m, \quad (27)$$

where

$$\begin{cases} M_1 &= \tilde{f}^T A_1 A_4 \tilde{f} + \tilde{f}^T A_4 H_1 \tilde{f} + \tilde{f}^T H_1^T A_4 \tilde{f}, \\ M_2 &= \tilde{f}^T A_1 A_4 \tilde{f} + \tilde{f}^T A_4 H_2 + H_2^T A_4 \tilde{f}, \end{cases}$$

which, written in total sum square form, becomes

$$M_1 = \sum_{i=1}^N a_{4i} \left( a_{1i} \tilde{f}_i^2 + 2a_{2i} (\alpha_i \tilde{f}_i^2 + \bar{V}_i \tilde{f}_i) \cdot \left( \sum_{k \neq i}^N \frac{\alpha_i \tilde{f}_i - \alpha_k \tilde{f}_k}{R_{ik}} \right) \right), \quad (28)$$

$$M_2 = \sum_{i=1}^N a_{4i} \tilde{f}_i^2 \left( a_{1i} + 2a_{2i} \alpha_i \left( \sum_{k \neq i}^N \frac{\bar{V}_i - \bar{V}_k}{R_{ik}} \right) \right). \quad (29)$$

Thus, we have

$$\begin{aligned} & M_1 + M_2 \\ &= \sum_{i=1}^N a_{4i} \left( 2a_{1i} \tilde{f}_i^2 + 2a_{2i} \left( \sum_{k \neq i}^N \frac{\bar{V}_i - \bar{V}_k}{R_{ik}} \right) \alpha_i \tilde{f}_i^2 \right. \\ & \quad + 2a_{2i} \left( \sum_{k \neq i}^N \frac{1}{R_{ik}} \right) \alpha_i^2 \tilde{f}_i^3 - 2a_{2i} \alpha_i \left( \sum_{k \neq i}^N \frac{\alpha_k \tilde{f}_k}{R_{ik}} \right) \tilde{f}_i^2 \\ & \quad + 2a_{2i} \left( \sum_{k \neq i}^N \frac{1}{R_{ik}} \right) \bar{V}_i \alpha_i \tilde{f}_i^2 \left. \right) \\ & \quad - \sum_{i=1}^N 2a_{4i} a_{2i} \bar{V}_i \left( \sum_{k \neq i}^N \frac{\alpha_k \tilde{f}_k \tilde{f}_i}{R_{ik}} \right). \end{aligned} \quad (30)$$

Arithmetic geometric mean inequality yields

$$\left| \frac{\alpha_k \tilde{f}_k \tilde{f}_i}{R_{ik}} \right| \leq \frac{1}{2} \left( \frac{\alpha_k \tilde{f}_i^2}{R_{ik}} + \frac{\alpha_k \tilde{f}_k^2}{R_{ik}} \right). \quad (31)$$

Substituting (31) in (30) yields

$$\begin{aligned} & M_1 + M_2 \\ & \geq \sum_{i=1}^N a_{4i} \left( 2a_{1i} \tilde{f}_i^2 + 2a_{2i} \left( \sum_{k \neq i}^N \frac{\bar{V}_i - \bar{V}_k}{R_{ik}} \right) \alpha_i \tilde{f}_i^2 \right. \\ & \quad + 2a_{2i} \left( \sum_{k \neq i}^N \frac{1}{R_{ik}} \right) \alpha_i^2 \tilde{f}_i^3 - 2a_{2i} \alpha_i \left( \sum_{k \neq i}^N \frac{\alpha_k \tilde{f}_k}{R_{ik}} \right) \tilde{f}_i^2 \\ & \quad + 2a_{2i} \left( \sum_{k \neq i}^N \frac{1}{R_{ik}} \right) \bar{V}_i \alpha_i \tilde{f}_i^2 \left. \right) \\ & \quad - \sum_{i=1}^N a_{4i} a_{2i} \bar{V}_i \left( \sum_{k \neq i}^N \frac{\alpha_k \tilde{f}_i^2}{R_{ik}} + \frac{\alpha_k \tilde{f}_k^2}{R_{ik}} \right). \end{aligned} \quad (32)$$

The last term in (32) can be written as

$$\begin{aligned} & \sum_{i=1}^N a_{4i} a_{2i} \bar{V}_i \left( \sum_{k \neq i}^N \frac{\alpha_k \tilde{f}_i^2}{R_{ik}} + \frac{\alpha_k \tilde{f}_k^2}{R_{ik}} \right) \\ &= \sum_{i=1}^N a_{4i} \left( a_{2i} \bar{V}_i \left( \sum_{k \neq i}^N \frac{\alpha_k}{R_{ik}} \right) \right. \\ & \quad \left. + \alpha_i \left( \sum_{k \neq i}^N \frac{a_{4k} a_{2k} \bar{V}_k}{a_{4i} R_{ki}} \right) \right) \tilde{f}_i^2. \end{aligned} \quad (33)$$

Therefore,

$$\begin{aligned}
& M_1 + M_2 \\
& \geq \sum_{i=1}^N a_{4i} \left( 2a_{1i} + 2a_{2i} \left( \sum_{k \neq i}^N \frac{\bar{V}_i - \bar{V}_k}{R_{ik}} \right) \alpha_i \right. \\
& \quad + 2a_{2i} \left( \sum_{k \neq i}^N \frac{1}{R_{ik}} \right) \alpha_i^2 \tilde{f}_i - 2a_{2i} \alpha_i \left( \sum_{k \neq i}^N \frac{\alpha_k \tilde{f}_k}{R_{ik}} \right) \\
& \quad + 2a_{2i} \left( \sum_{k \neq i}^N \frac{1}{R_{ik}} \right) \bar{V}_i \alpha_i - a_{2i} \bar{V}_i \left( \sum_{k \neq i}^N \frac{\alpha_k}{R_{ik}} \right) \\
& \quad \left. - \alpha_i \left( \sum_{k \neq i}^N \frac{a_{4k} a_{2k} \bar{V}_k}{a_{4i} R_{ki}} \right) \right) \tilde{f}_i^2. \tag{34}
\end{aligned}$$

Thus, a feasible region for  $\alpha_i$  is that,

$$\begin{aligned}
\Omega_{\alpha_i} = & \left\{ \alpha_i \in \mathbb{R} \left| 2a_{1i} + 2a_{2i} \left( \sum_{k \neq i}^N \frac{\bar{V}_i - \bar{V}_k}{R_{ik}} \right) \alpha_i \right. \right. \\
& + 2a_{2i} \left( \sum_{k \neq i}^N \frac{1}{R_{ik}} \right) \alpha_i^2 \tilde{f}_i - 2a_{2i} \alpha_i \left( \sum_{k \neq i}^N \frac{\alpha_k \tilde{f}_k}{R_{ik}} \right) \\
& + 2a_{2i} \left( \sum_{k \neq i}^N \frac{1}{R_{ik}} \right) \bar{V}_i \alpha_i - a_{2i} \bar{V}_i \left( \sum_{k \neq i}^N \frac{\alpha_k}{R_{ik}} \right) \\
& \left. \left. - \alpha_i \left( \sum_{k \neq i}^N \frac{a_{4k} a_{2k} \bar{V}_k}{a_{4i} R_{ki}} \right) \geq 0 \right\}. \tag{35}
\end{aligned}$$

Therefore, for any  $\alpha_i \in \Omega_{\alpha_i}$ , we have  $\dot{W} < 0, \forall [f, \tilde{P}_m] \neq 0$  and as a conclusion, the nonlinear system (11) is asymptotically stable. Moreover, once  $\alpha_i$  are determined, we can get an estimate of the region of attraction  $\Omega_c$  for the state variables:

$$\begin{aligned}
\Omega_c = & \left\{ [f, \tilde{P}_m] \in \mathbb{R}^{2N} \left| \sum_{k \neq i} \frac{-\alpha_i \tilde{f}_i + \alpha_k \tilde{f}_k}{R_{ik}} \leq \frac{a_{1i}}{\alpha_i a_{2i}} \right. \right. \\
& - \left( \sum_{k \neq i}^N \frac{\bar{V}_i - \bar{V}_k}{R_{ik}} \right) - \left( \sum_{k \neq i}^N \frac{1}{R_{ik}} \right) \bar{V}_i \\
& - \frac{\bar{V}_i}{2\alpha_i} \left( \sum_{k \neq i}^N \frac{\alpha_k}{R_{ik}} \right) \\
& \left. \left. - \frac{1}{2a_{4i} a_{2i}} \left( \sum_{k \neq i}^N \frac{a_{4k} a_{2k} \bar{V}_k}{R_{ik}} \right), i = 1, \dots, N. \right\} \tag{36}
\end{aligned}$$

It is not easy to use (35) and (36) directly to get a feasible region due to their complicated expressions. Though a feasible region can be easily found by the linear method (19), we can only approximate the nonlinear system (11) by its linearization in a small neighbourhood of the origin, of which we do not know the size. Thus, when determining the gains  $\alpha_i$ , we need to combine these two methods together.

TABLE I

PARAMETER VALUES OF EACH AC AREA ('-' MEANS DIMENSIONLESS).

Parameter	Area					Unit
	1	2	3	4	5	
$f_{nom}$	50	50	50	50	50	Hz
$P_m^o$	50	80	50	30	80	MW
$P_{nom}$	50	80	50	30	80	MW
$J$	2026	6485	6078	2432	4863	kg m <sup>2</sup>
$D_g$	48.4	146.3	140.0	54.9	95.1	W · s <sup>2</sup>
$\delta$	0.02	0.04	0.06	0.04	0.03	-
$T_{sm}$	1.5	2.0	2.5	2	1.8	s
$P_l$	100	60	40	50	40	MW

In general, the feasible region obtained by linear method is larger than the nonlinear method. At first, we use linear method to get a feasible value for  $\alpha_i$ , then we put it into (35) and (36) to see if this value satisfies the nonlinear method's condition to stabilize our system in the domain of interest, i.e.  $\tilde{f}_i \in [-1, 1]$  for  $i = 1, \dots, N$ . If this is not the case, we choose a smaller value for  $\alpha_i$  and verify if it satisfies (35) and (36). We repeat this procedure until a proper  $\alpha_i^*$  appears.

The feasible region of the controller gain  $\alpha$  given in this paper depends on the choice of Lyapunov function. The one used in this paper was chosen for two reasons. First, as can be seen in (18), there is no cross term ( $\tilde{f}^T \tilde{P}_m$ ), which greatly simplifies the calculation. Second, the feasible region thus obtained is not so small. However, the feasible region of the controller gain is only a sufficient condition, which guarantees ultimate boundedness of the closed-loop system. Thus, with an  $\alpha$  outside this feasible region, the system does not necessarily become unbounded.

#### IV. SIMULATIONS

The controller studied in the previous section is tested by computer simulations. The simulated example concerns an MTDC grid of 5 AC areas, whose parameter values are presented in Table I. The system is supposed to initially operate at the reference operating point. Then at time  $t = 2$  s, the load demand of AC area 2 has a step increase by 30%.

Figs. 2 and 3 illustrate the frequency and the mechanical power response without any controller, i.e.  $\alpha_i = 0$ . In Fig. 2, the minimum value of  $f_2$  is less than 49 Hz, which is beyond frequency safety range  $50 \pm 1$  Hz, and the final value is 49.5615 Hz. The peak value of  $P_{m2}$  is nearly 106 MW and the final value is nearly 97.6 MW.

Figs. 4 and 5 illustrate the frequency and the mechanical power response when the controller is implanted. Table II shows the values for  $\alpha$  calculated by LMI techniques. The proposed  $\alpha$  are in their feasible region that can make sure that the system is stable. Note that, the minimum value of  $f_2$  is between 49.4515 Hz and 49.452 Hz which is in the safety range and the final value  $f_2$  is 49.7299 Hz.  $P_{m2}$  has a peak value of nearly 92.5 MW, and is stabilized at 91 MW. The above results show that our controller makes a significant improvement for frequency not only in the transient performance but also in the steady-state performance.

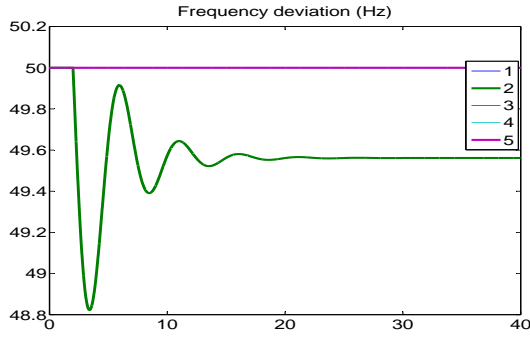


Fig. 2. Frequencies of 5 AC areas without any controller.

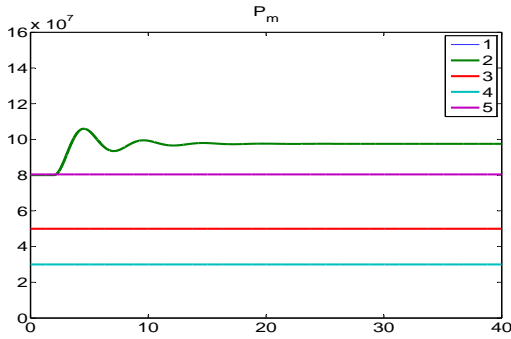


Fig. 3. Mechanical power inputs of 5 AC areas without any controller.

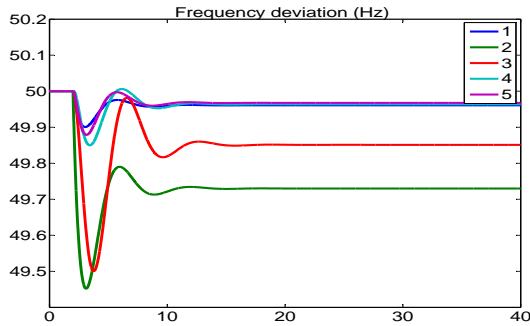


Fig. 4. Frequencies of 5 AC areas with controller.

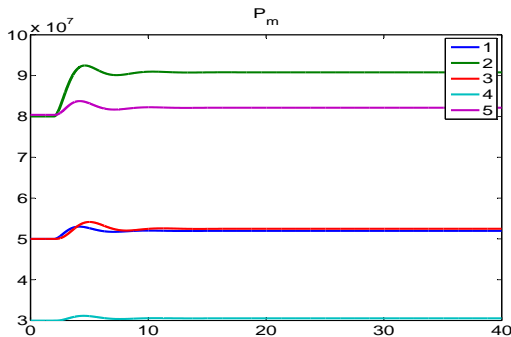


Fig. 5. Mechanical power inputs of 5 AC areas with controller.

TABLE II

VALUES OF  $\alpha_i$  CALCULATED BY LMI.

$\alpha_1$	$\alpha_2$	$\alpha_3$	$\alpha_4$	$\alpha_5$
1700	397	185	548	868

## V. CONCLUSIONS

In this paper, we addressed the problem of developing a controller that shares primary reserves between the AC areas connected by a multi-terminal HVDC system. In the case of a power imbalance, the controller reduces the burden of the affected AC area by making the other AC areas collectively react to that disturbance. For this, we study a control law which is only based on local measurements and does not need communication, thus avoiding the disadvantages caused by time-delay. For this control law, a sufficient condition is found to determine a feasible region for the controller gain, which guarantees that the multi-terminal HVDC grid is ultimately bounded. Simulation results shows that these local controllers achieve the objective of sharing primary reserve and keep the system ultimately bounded.

In our case, we just consider one AC area connected to one converter. In the future, we can extend our system by connecting an AC area with several converters. In this case, more than one DC grid are involved in frequency regulation. We need to study how to modify the controller to achieve the objective of sharing primary reserves while maintaining the stability of the system.

## REFERENCES

- [1] P. Kundur, *Power System Stability and Control*. McGraw-Hill, 1994.
- [2] A. Hamzei-nejad and C. M. Ong, "Coordinating the DC power injections of a multiterminal HVDC system for dynamic control of AC line flows," *IEEE Transactions on Power Systems*, vol. PWRS-1, May 1986.
- [3] J. Dai, Y. Phulpin, A. Sarlette, and D. Ernst, "Impact of delays on a consensus-based primary frequency control scheme for AC systems connected by a multi-terminal HVDC grid," in *Proceedings of the 2010 IREP Symposium - Bulk Power Systems Dynamics and Control - VIII*, (Buzios, Rio de Janeiro, Brazil), 1-6 August 2010.
- [4] J. Dai, Y. Phulpin, A. Sarlette, and D. Ernst, "Voltage control in an HVDC system to share primary frequency reserves between non-synchronous areas," in *Proceedings of the 17th Power Systems Computation Conference (PSCC-11)*, (Stockholm, Sweden), 22-26 August 2011.
- [5] H. Khalil, *Nonlinear System*. Prentice Hall, 1996.
- [6] A. Isidori, *Nonlinear Control Systems*. Springer Verlag, 1995.
- [7] R. Marino and P. Tomei, *Nonlinear Control Design - Geometric, Adaptive and Robust*. Hemel Hempstead, London: Prentice Hall, 1995.
- [8] J.-J. Slotine and W. Li, *Applied Nonlinear Control*. Prentice Hall, 1991.
- [9] S. Boyd, L. E. Ghaoui, E. Feron, and V. Balakrishnan, *Linear Matrix Inequalities in System and Control Theory*. SIAM, Studies in Applied Mathematics, 1994.